CERN-LHCC-2021-025 / CMS-TDR-024
25/11/2021

A Run 4 Zero Degree Calorimeter for CMS

Y. Bashan[a], Z. Citron[a], B. Cole[b], M. Grosse Perdekamp[c], A. Hase[d], T. Koeth[e], C. Lantz[c], S. Lascio[e], R. Longo[c], D. MacLean[c], A. Mignerey[e], Y. Moyal[a], M. Murray[d], M. Nickel[d], M. Phipps[c], S. Popescu[d], N. Santiago[c], A. Sickles[c], S. Shenkar[a], P. Steinberg[f], L. Sudit[a], A. Tate[c], Q. Wang[d], and S. Yang[c]

[a]Ben-Gurion University of the Negev, Dept. of Physics, Beer-Sheva 84105, Israel
[b]Columbia University, Dept. of Physics, New York, NY 10027, USA
[c]University of Illinois at Urbana-Champaign, Dept. of Physics, Urbana, IL 61801-3080, USA
[d]University of Kansas, Dept. of Physics, Lawrence, KS 66045, USA
[e]University of Maryland, Dept. of Chemistry and Biochemistry, College Park, MD 20742, USA
[f]Brookhaven National Laboratory, Upton, NY 11973, USA

Abstract

The Run 4 Heavy Ion program of the LHC offers great physics opportunities to CMS and ATLAS. The ZDCs are increasingly important for characterizing A+A , p+A , γ+A and γ+γ collisions, particularly the impact parameter between the colliding particles. However, the increasing LHC luminosity places a significant strain on the current ZDC design, and the space in the absorber region will be reduced by a factor of two, requiring all new detectors for LHC Run 4. Recent developments in rad-hard materials allow the construction of compact rad-hard fast ZDCs to fully exploit the potential for QED and QCD physics during Run 4. In this proposal, groups from ATLAS and CMS are collaborating to produce high-performance, cost-effective ZDCs for this new era. This document describes scientific motivation for the project and the CMS specific aspects.

November 25, 2021

Contents

1 Scientific Motivation

Zero Degree Calorimeters (ZDC) have played a central role in the success of CMS Heavy Ion program [12, 9, 2, 4, 5, 17]. To a good approximation all HI papers - rely on the ZDC for triggering and pileup suppression. In fact, the number of analyses in which the ZDC plays an important role in the offline analysis, e.g. for distinguishing peripheral and ultra-peripheral collisions, has increased recently and includes many analyses currently in progress, including photonuclear dijets and forward rapidity gaps [3].

This document explains how the next generation of ZDC detectors can exploit future opportunities for high-density QCD and photon-photon phyiscs at the HL-LHC in Ref. [8]. Running at the higher luminosities, just as in the earlier runs, will require the ability to categorize the events as hadronic, photon-nucleus or photon-photon in real time. Thus, a ZDC that can handle the rates and decreased bunch spacing is of highest priority. In addition, debates in cosmic ray physics, as well as the observation of flow in small systems has led to an increased interest in studying reactions between light ions ($A < 50$).

The high luminosity upgrade of the LHC will also lead to modifications of the beam optics. The point where the clockwise and anticlockwise beam merge, known colloquially as the “pair of pants" will move 13m closer to the interaction point (IP). The absorber for neutral particles known by its french acronymn, TAXN, has been redesigned to accommodate the reduced distance between the beam pipes, [11, 10]. The constraint of the beam pipes implies a much narrower space for the ZDCs, which will require a completely new design. Our group has worked very closely with the HL-LHC group on the design of the TAXN, the ZDCs and auxiliary equipment such as cranes. The result is a detector that can be very easily installed and reach the physics goals described above.

A joint ZDC calorimeter project (JZCaP) began in 2017, as a collaboration between the ATLAS and CMS ZDC efforts. We note that this is the first ATLAS-CMS collaborative detector effort. The ongoing goal of JZCaP is to design a detector capable of withstanding the rates and radiation doses expected after the HL upgrade of the accelerator in Run 4 and improving its performance for physics measurements. The characterization of collision geometry will be improved with the implementation of a newly-designed RPD to be installed in both ATLAS and CMS. The identification and measurement of energetic photons emitted at forward rapidity will be improved thanks to a newly designed segmented electromagnetic section of the ZDC.

The Run 4 ZDC has been designed jointly by the ATLAS and CMS in very close collaboration with the HL-LHC group. Using a common design in Run 4 for the two collaborations will lead to positive synergies in detector development and to the consistent applications of algorithms used for the characterization of different event classes, as well as to lead to better understanding of relevant systematic effects. This will allow for a more straightforward comparison of physics results obtained by the two collaborations analyzing Run 4 data. Moreover, the dramatically-improved radiation hardness of the detector readout system will result in increased stability of the detector response during the HI runs and in greater flexibility regarding the possibility of HI data-taking during modest-intensity pp running.

The primary purpose of the ZDCs for both ATLAS and CMS is to detect far forward neutral particles ($|\eta| >$8.3 in Run 1-3, > 8.5 in Run 4 and 5). This is primarily used to detect "spectator" neutrons, which do not participate directly in hadronic heavy ion collisions. In tandem with substantial energy in the central detector, a two sided ZDC topology is a clear tag of a hadronic collision and thus provides a useful trigger signature.

Beyond triggering, the measurement of these neutrons can be used in characterizing the geometry of observed interactions. In hadronic processes, the correlation of the ZDC energies with hadronic transverse energy measured in the central region reflects the impact parameter between the two nuclei, while their orientation reflects the reaction plane of the collision. The ZDCs can also measure the reaction plane of heavy ion collisions. This can help to extract information on the bulk viscosity of the quark gluon plasma and initial fluctuations in the nuclear wave-function.

Conversely, selecting events with only one (or neither ZDC with a substantial signal, corresponding to one or more neutrons, is a powerful way to trigger on non-hadronic interactions. Non-hadronic processes, often collectively referred to as Ultra-Peripheral Collisions (UPC), are electromagnetic interactions of the ions, *i.e.* interactions involving the nearly-real photons associated with the relativistic ion. A photon from one ion may interact with the other ion's coherent nucleus in photo-nuclear interactions, sometimes even producing pairs of jets [1]. In other cases, the photon may interact with associated photons of the opposite ion, leading to a rich phenomenology of photon-photon interactions. See [13] for a recent review of both one and two photon processes. A one-ZDC trigger provides the most straightforward way to acquire an unbiased sample of these events.

Selecting low multiplicity events and then requiring both ZDCs to show no signal, is a clean way to enhance photon-photon processes. However, it should be noted that not all photon-photon events are associated with no activity in the ZDCs. Although this is true at leading order, the number of neutrons in each ZDC is also correlated with the impact parameter, as this controls the flux of secondary soft photons which can break up one or both nuclei, and control the number of emitted neutrons. Figure 1 shows distributions from muon pairs produced by photon-photon collisions, and characterized by CMS by the angular separation $\Delta\phi$ between the two muons, represented as an acoplanarity $\alpha = 1 - |\Delta\phi|/\pi$. Both the mean acoplanarity and the invariant mass of the muon pair increase as the neutron multiplicity increases. This reflects a negative correlation between the internuclear impact parameter and the transverse momenta of the photons. The closer the nuclei, the the more the photon transverse momenta increase, as does the probability of a secondary photon emission exciting one or both nuclei to emit several neutrons.

The extremely strong EM fields of the LHC accelerated beams, and especially the ion beams, serve as a very bright source of high energy photons. The ZDCs are efficient tags of photon-photon and photon-nucleus collisions. One of the earliest predictions of quantum electrodynamics was the scattering of light-by-light (LbyL). The observation of such scattering

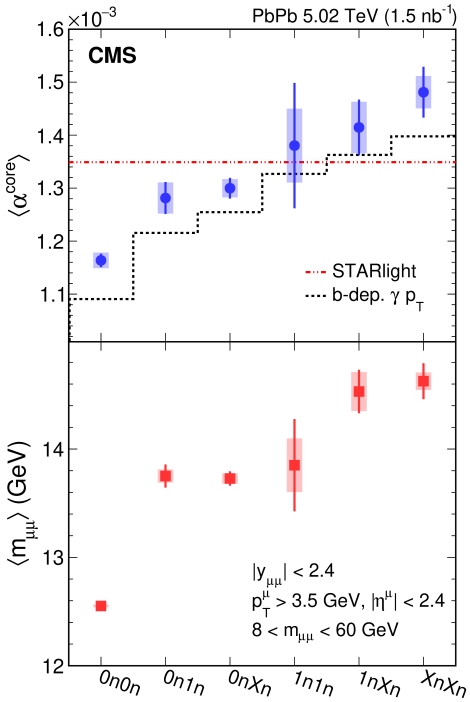

Figure 1: Neutron multiplicity dependence of width of the acoplanarity of the two muons $\langle \alpha^{\mathrm{core}} \rangle$ (upper) and the invariant mass $\langle m_{\mu\mu} \rangle$ (lower) of $\mu^+\mu^-$ pairs in ultraperipheral Pb+Pb collisions at $\sqrt{s_{NN}}$= 5.02 TeV. The vertical lines on data points depict the statistical uncertainties, while the systematic uncertainties of the data are shown as shaded areas. In the upper plot, the dashed-dot (red) line shows the STARlight prediction, and the dotted (black) line corresponds to the leading-order QED calculation.

is possible using the photons generated by the LHC beams [16]. Besides its significance in the context of QED, LbyL scattering may be sensitive to possible beyond the standard model physics.

The LbyL process is dependent upon loop diagrams shown in Fig. 2. If new physics is present, additional loop diagrams may be present which would change the light-by-light rate. The present data has already been used to set limits on axion like particles that couple to electromagnetism [14].

The photo-production of tau pairs allows a clean search of new physics. Through diagrams similar to those in Fig. 2 new particles may increase the production rate and modify the kinematics of τ pairs. This search is motivated by recent theoretical and experimental advances in g-2 for the muon. Both LbyL and tau g-2 studies are currently statistics limited. The ZDCs are essential for this physics in Runs 3 and 4.

The Run 4 ZDC will include a reaction-plane detector (RPD) which will allow an estimate of the reaction plane angle of individual HI collisions from the correlated deflection of the spectator neutrons. It will be possible to extract all the higher-order harmonics (v_n, $n \geq 2$) using the $n = 1$ reaction plane reflected by the nuclear fragments, the plane most correlated with the early stages of the collision. It will then be possible to compare the results with those obtained by the two experiments using the event plane determined in the central detector. Taking data with the RPD for different size ions will open the possibility to scan the A-dependence of the directed flow a feature, directly related to the compressibility of the nuclear matter [6].

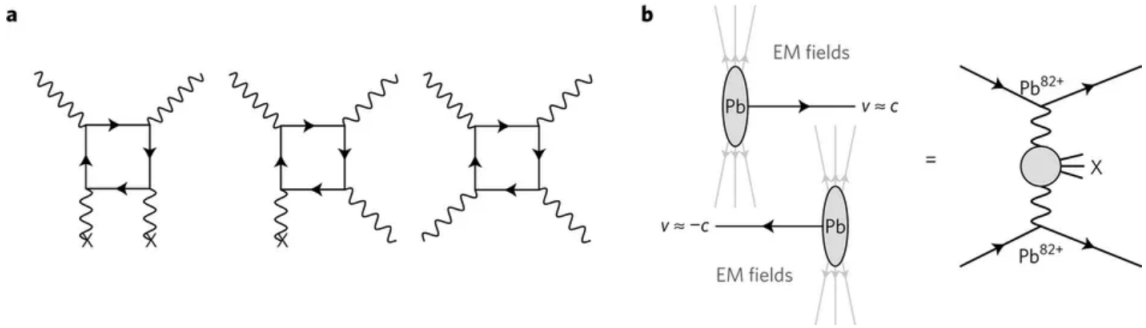

Figure 2: **a**: Diagrams for Delbrück scattering (left), photon splitting (middle) and elastic LbyL scattering (right). Each cross denotes external field legs, for example, an atomic Coulomb field or a strong background magnetic field. **b**: Illustration of an ultra-peripheral collision of two lead ions. Electromagnetic interaction between the ions can be described as an exchange of photons that can couple to form a given final state X. The flux of photons is determined from the Fourier transform of the electromagnetic field of the ion, taking into account the nuclear electromagnetic form factors.

2 Detector Design

The new detector is expected to have very similar energy resolution as the current ZDCs and sufficient spatial resolution to allow the reconstruction of the first order reaction plane.

The measurement of the single-neutron peak is the primary tool used to calibrate the energy scale of the calorimeter. The single-neutron resolution is limited physically by 1) the Fermi momentum broadening of the neutrons in the incident nuclei and 2) by the energy containment of the showers. In Run 2 these resulted in a fractional resolution of about 16-17%. The greater hadronic depth of the proposed calorimeter will reduce the punch-through contribution to the single-neutron energy response, but that will be partly offset by increased transverse leakage due to narrower width.

The ZDC will installed in between the two beam pipes in the Target Absorber for Neutrals (TAXN), passive components of the accelerator designed to protect the nearby superconducting magnets from the forward neutral radiation coming out from the interaction region (IR). The TAXN will located at ± 130 m from the interaction point, at the place where the long straight-section of the beam-pipe branches back into two independent beam-pipes.

In addition to the geometrical constraints the radiation field will be much higher in Run 4 and the tunnel will be much more crowded with new cables and alignment systems. The limited space for maneuvering the detector imposes the requirement that the detector should be a single module, with minimal mass. Furthermore, the number of connectors should be reduced to the absolute minimum possible, with straightforward access.

The ZDC, will use tungsten interleaved with fused silica rods as the active medium. Photons and neutrons hitting the tungsten generate a shower of particles. Charged shower particles with velocities above the Cherenkov threshold generate light in the rods. Light emitted out of the top of the rods is reflected by an air light-guide towards the window of a Photo Multiplier Tube (PMT), which converts the light into an electrical pulse.

The Run 4 ZDC will be a single module comprised of EM, RPD and Had sections, see 3. The EM and HAD sections are fused silica-tungsten sampling calorimeters with different sampling ratios, while the RPD will be either an array of fused-silica tile or fibers of different length.

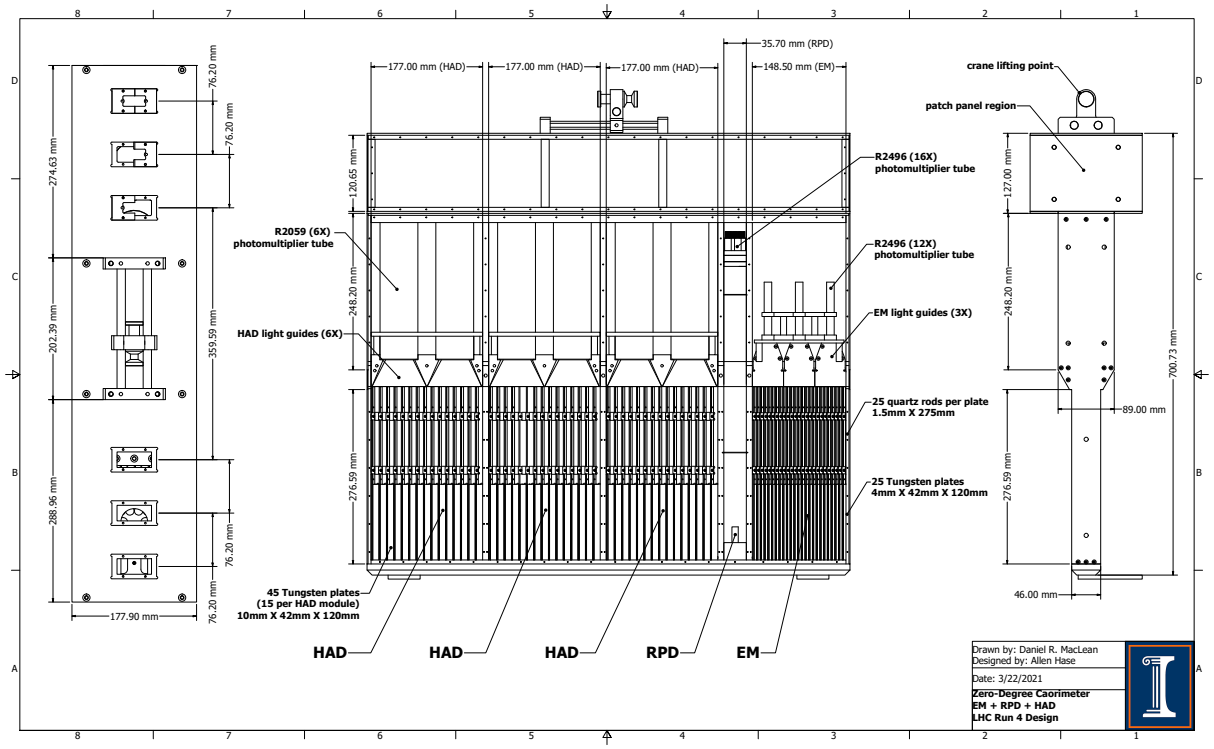

Figure 3: CAD drawing of the ZDC.

2.1 ZDC electromagnetic section

The EM section, shown in Fig. 4, is the first part of the ZDC encountered by particles impinging on its front face. The active region consists of layers of fused silica rods (25 each of 1.5 mm diameter and 275 mm height), alternating with tungsten (W) plates (each $42 \cdot 120$ mm^2 in the x-y plane, and 4 mm thick).

Above the tungsten plates, the fused silica rods are guided by stainless steel plates located atop the tungsten, with the same dimensions in x and z, and a height of 148 mm.

The ZDC EM section has a 4-fold horizontal segmentation and 3 longitudinal sub-sections. As CMS experience demonstrates, the x segmentation can be used to determine the average incident beam position, e.g. for horizontal crossing angles. Combining horizontal and longitudinal segmentation will allow for a 2D mapping of the shower in the EM section, allowing discrimination between neutrons and photons, especially in tandem with the information from the RPD (described in the next section). The EM segmentation is implemented by the light-guide assemblies.

2.2 Reaction Plane Detector (RPD)

The RPD is installed immediately downstream of the EM module, in a 3.5 cm long slot defined by two structural walls of about 9 mm thickness each. We are currently considering two versions of the RPD, either using tiles or a pan flute design based on fibers. The PF RPD design is shown in Fig. 5.

The active region of the PF RPD is comprised of 256 overlapping fibers that can be treated as a virtual 4×4 array of square tiles which provide spatial sensitivity to incident charged particles in the $x-y$ plane.

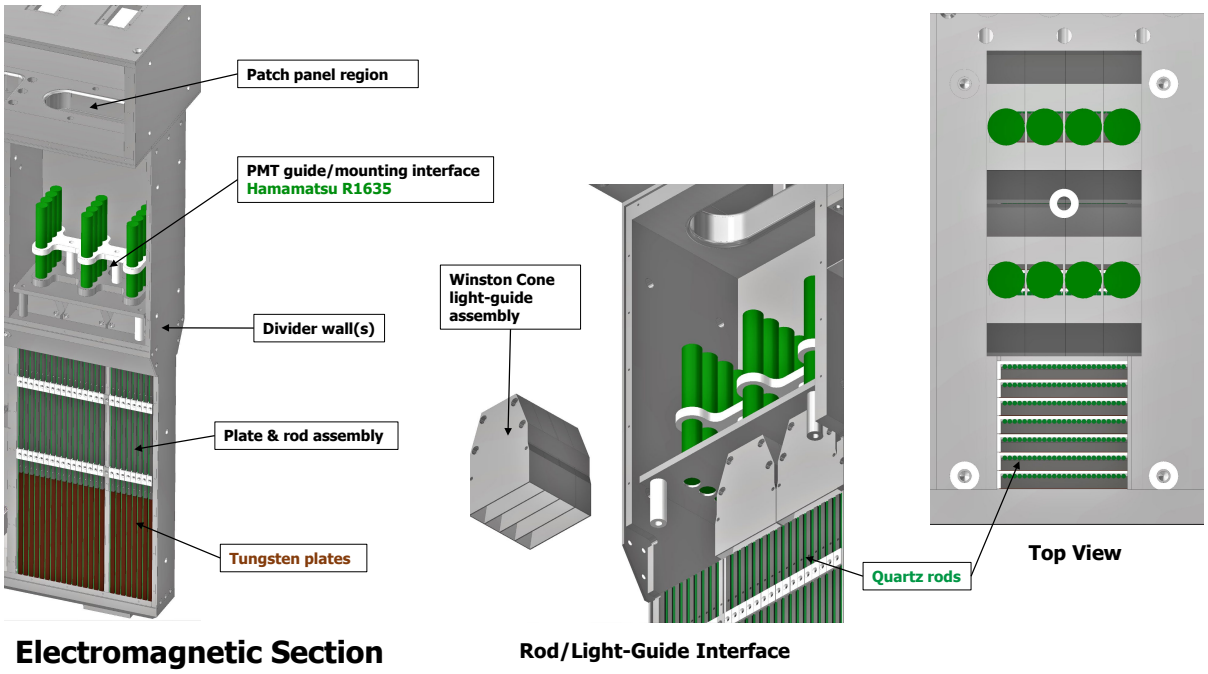

Figure 4: CAD drawing of the EM section of the ZDC detector. For better visibility, the top view on the right does not include the patch panel components.

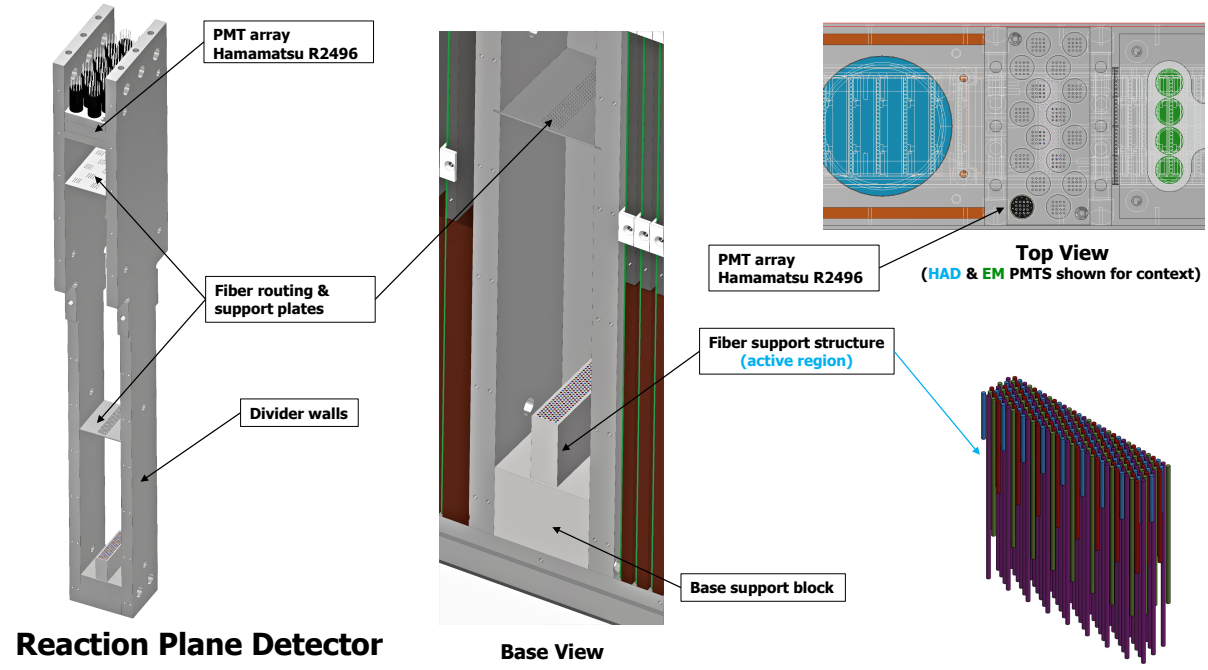

Figure 5: Design drawing of the RPD section of the ZDC detector. The RPD fibers above the active region are not shown for better visualization.

2.3 Hadronic section

The hadronic section has a total of 4.5 nuclear interaction lengths, read out by six photomultipliers. The fused silica rods are sandwiched between 10 mm tungsten plates with x-y transverse dimensions equal to 42×120 mm^2. The rods terminate at an air light-guide which redirects the photons toward the PMT.

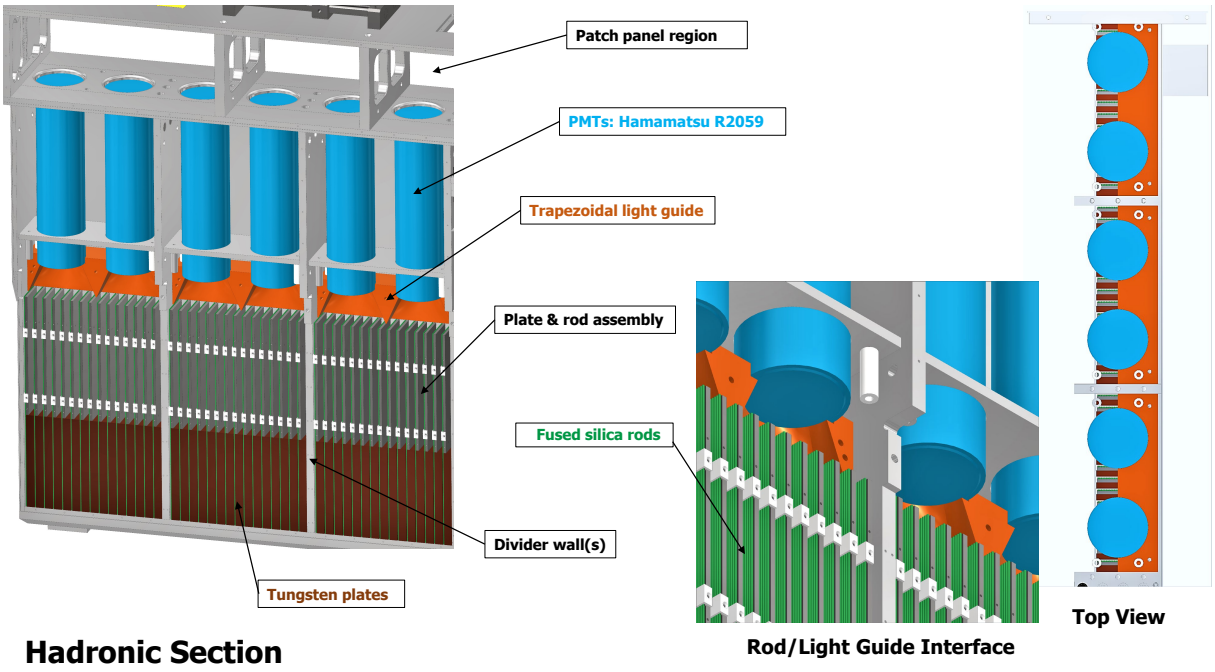

Figure 6: CAD drawing of the HAD section of the ZDC detector. For better visibility, the top view on the right does not include the patch panel components.

2.4 Fused silica rods

Several different kinds of fused silica doped with with different concentration of OH or H_2 has been tested by insertion in the BRAN luminosity monitor. The radiation hardness of these rods has been measured up to 500 GRad. This 100s of times greater than the doses possible for heavy ion running and corresponds to about 25 femto barn of pp running. This should allow the ZDCs to be inserted for special runs such as the XeXe run in 2017, even if the ZDCs cannot be removed immediately. It should be noted that the fact that the current ZDCs could not be inserted for XeXe resulted in a significant loss of physics results.

In parallel, studies of activation have shown that calculations of the dose rates by the LHC radiation simulation group are accurate to within 20%. The range of these studies will be increased by and order of magnitude using both reactor tests and insertion of rods into empty slots with the BRAN detectors at CMS and ATLAS. This should allow a final decision on which rods to use well before Run 4. The light yield of the rods was tested in a realistic environment using a test beam. The analysis of this data is ongoing.

2.5 Expected performance

A key parameter to determine the performance of the ZDC is the shower containment. The negative impact of the reduction in width has been compensated for by increasing the depth of the detector and making the ZDC one continuous piece. (Currently the BRAN luminosity monitor separates the EM and hadronic sections).

The Run 4 ZDC will be only 1/2 as wide as the current ZDCs. On the other hand the detector is longer and is in one piece. For Run 3 the LHC BRAN luminosity monitor was placed between the electromagnetic and hadronic sections of the ZDC. This gap produced some shower leakage. The impact of these changes on the containment of the ZDC was investigated studying the energy deposited (E_{dep}) by 2.51 TeV neutron events in all the ZDC modules. The

E_{dep} distribution was then fitting with a Gaussian distribution, to calculate the mean ($\overline{E_{cont}}$) and the standard deviation ($\sigma_{E_{cont}}$). The resolution for 2.5 TeV neutrons hitting the center of the detector was found to be equal to that of the current detector, resulting in a resolution of 18% for the one neutron peak.

The performance of the ZDC also depends on the beam tuning at the interaction points (IPs). For a horizontal crossing angle, at angles greater than $\sim$120 μrad the energy containment begins to fall off sharply. A request for vertical crossing angles at both experiments during heavy ion running was made to the LHC Heavy Ion beams team. Recent calculations suggest this is possible [7].

Figure 7 summarizes the CMS Tile RPD performance for position measurements. The left hand panel of Fig. 7 shows that correlation between the average X of the signal in the RPD and that of the EM section of the ZDC. There is a very clear linear relationship between the two. The mean X value is displaced from 0 due to the fact that CMS has a horizontal crossing angle. Note that the EM section is divided into 5 strips in X and so has no sensitivity to the distribution of neutrons in the Y direction. The right hand panel of Fig. 7 shows the difference the average X position of the signal in the RPD compared to that expected from the electromagnetic part of the CMS ZDC. From a fit to the distribution in the right in we estimate that the tile RPD has an x resolution of 1.6 mm.

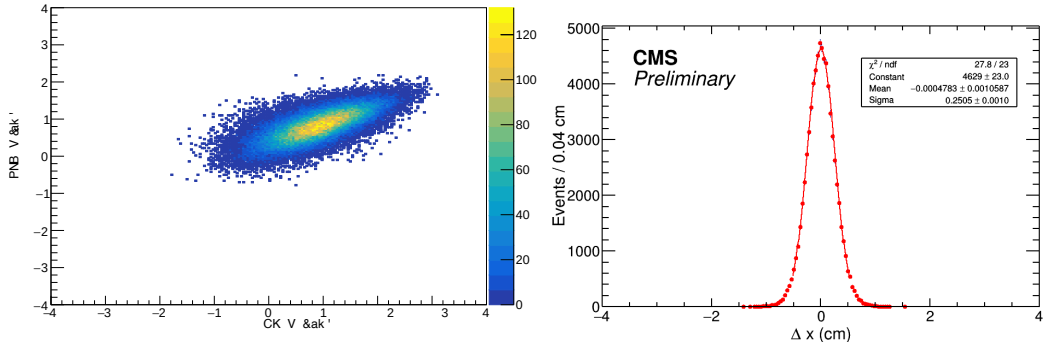

Figure 7: Comparison of the average X of the signal in cms f the CMS tile PRD EM section of the ZDC for 2018 PbPB in the centrality range 30-40%. Left panel: Event by event distribution for the average X of signal in the RPD versus the average X in the EM section. Right panel: The difference in X between RPD and the value predicted from the left hand panel.

Directed flow tends to lead to correlated deflection of all of the neutrons in each event, with neutrons in opposing directions emitted opposite in azimuth relative to one another. A simple generation mechanism was implemented to introduce directed flow. Event-by-event fluctuations in the number of the neutrons were obtained by sampling a Poisson distribution with a mean of say 30. Each neutron was given a three-dimensional Fermi momentum and a p_T kick along direction of the reaction plane, p_T^{spec}. The neutrons are then boosted by the beam moment and injected in the Geant4. A convolutional neural network (CNN) algorithm was chosen to perform the pattern recognition on the PF RPD signals. The results are shown in Fig. 8 and show a resolution sufficient for the expected physics.

3 Integration into CMS

The integration strategy to both generate High voltage and digitize signals in the dedicated bunkers in the near the TAXN. This reduces noise and allows for complete galvanic separation

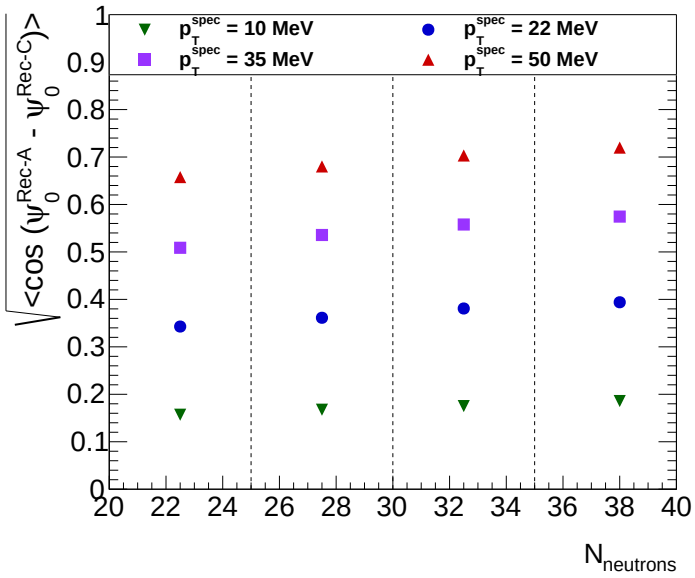

Figure 8: Simulated reaction plane resolution estimated using the two sub-reaction planes [15] measured by the two arms of the ZDC. The results are presented for four different simulations where the transverse momentum kick along the direction of the reaction plane, p_T^{spec}, was varied. The vertical dashed lines correspond to the limits of the four bins in neutron multiplicity where the resolution was evaluated. Statistical uncertainties are smaller than the markers.

of the ZDCs for USC55. All data transfer and detector control will be provided through optical links. The ZDC electronics is based on that of HCAL and follows the HCAL upgrade path. For Run 4 the high voltage supplies will be upgraded to modern CAEN units.

For the 2018 Pb+Pb run, the ZDC signals were digitized in a readout mini crate on each side of CMS in the LHC tunnel, see Fig. **??**. The readout mini crate consists of a control module (ngCCM), and two digitize modules (QIE10). Each QIE10, identical to the CMS Hadronic forward (HF) front end electronics, can process 24 channels with LEMO analog input interfaces.

The control and data links of the mini crate were recently upgraded to multi-mode optical fibers for the very successful pilot run in October 2021. The fiber patch panel is located at the top of the readout crate. The readout mini crate is powered by a LV power supply, which is controlled by an analog cable to reset the power. It is important to isolate the LHC tunnel ground from the ground of the counting room. The total power consumption of each mini crate is estimated to be less than 80W.

The digital data produced by the QIE10s are collected by the μHTR back-end card. The μHTR card can provide certain trigger decisions for event triggering based on the ZDC signals, which will be used for CMS L1 trigger system.

The overall data acquisition and trigger system is very similar to the CMS Hadronic Forward (HF) detector. This has the great advantage that for detector control and safety (DCS), data acquisition event reconstruction (DAQ), and data quality monitoring (DQM) the ZDC is just another subsystem of HCAL and so benefits from central support. This will continue in Run 4. The HCAL back end electronics uses Fully Programmable Gate Arrays (FPGAs) to search for jets. The ZDC group, in collaboration with other HCAL members, has adapted this system to trigger on single neutrons. We are continuing to improve the quality and stability of this trigger.

Since the ZDC signals are digitized very close to the detector the electronic noise is very low, corresponding to less 1/2% of the single neutron peak. The ZDC signal does have a dependence

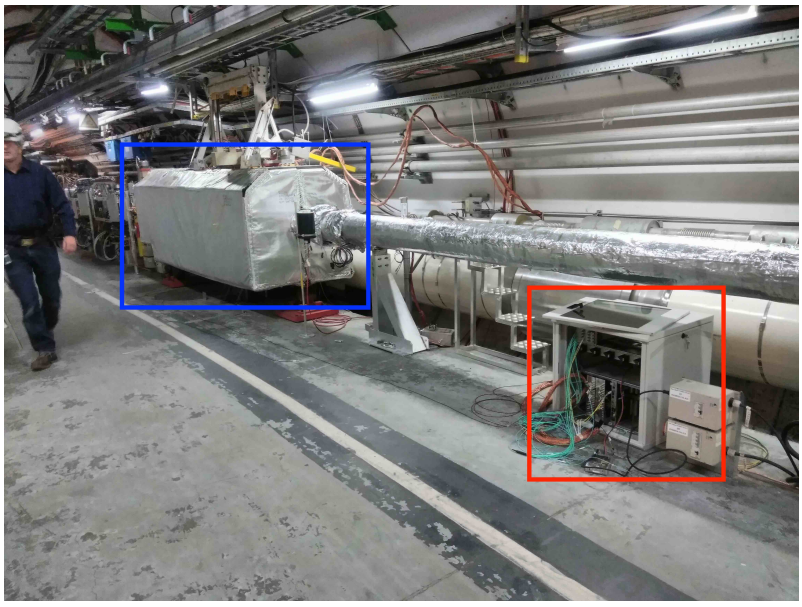

Figure 9: The CMS ZDC located inside the TAN in blue box, and the front end electronics inside the mini crate in red box. Photo taken during the 2018 PbPb heavy ion run preparation.

upon the instantaneous luminosity, with the single neutron peak varying by about 8% during a typical LHC store. This is corrected offline and seems to be mainly a pileup effect. For Run 4 the clock frequency of the HCAL electronics will double, allow better pileup rejection.

One complication for Run 2 was the need to replace the optical fibers of the ZDC readout each year, since they suffered radiation damage during the pp running time. For Run 3 and 4 this effect will be eliminated by moving the electronics into very well shielded bunkers close to the ZDCs. This will simplify setting up the ZDCs before each run. For Run 4 our target is to have all the ZDC electronics working within 24 hours of the ZDC installation, leaving only a final timing check once the heavy ion beam starts. This will allow the ZDCs to take data within the first day of heavy ion beams.

The offline software for Run 4 will be based on that used for Run 3. The calibration is based on the single neutron peak which we expect to be stable throughout a typical run. Pileup rejection will be implemented via a template fit to the time profile of the signal.

4 Budget

The cost of the project is $1.8M which rises to $2.4M after inflation (2.5% a year) and contingency. These costs will be born by the DOE Office of Nuclear Physics. Construction funding is expected to start in 2023 and continue for four years, with peak funding in 2025. The DOE funding will be used to construct four ZDC and to establish the relevant infrastructure to install and operate the detector in the HL-LHC. An engineer will be associated to the project for four years at 0.25 FTE. The final goal is to have the four ZDCs constructed and certified by the CERN transport group in the first quarter of 2027, to then test all the detectors using the CERN test beam facilities at the SPS before installation underground.

The cost and schedule for the joint ZDC Upgrade project have been developed using engineering estimates, vendor quotes and experience from the construction of the current ZDCs from the corresponding ATLAS and CMS groups. About one-third of the cost of the project is for the construction of the four ZDCs. Other costs are for electronics, cables, HV system,

cranes and modification of the TAXN specifically for the ZDC.

Four different levels of budget contingency have been chosen, based on the available documentation for the cost estimate:

- Available quote: 10%.
- Previous purchase: 15%.
- Catalogue value: 20%.
- Engineering or expert estimate: 40%

5 Schedule

The schedule for the construction, testing, and installation of the ZDCs is as follows:

- 2023: beginning of the DOE project. Finishing of the final design, construction of the first, fully-functional "pre-production" ZDC begins.
- 2024: completion of the "pre-production" ZDC construction potentially with inexpensive quartz, but with production-quality absorber and PMTs. Testing in the SPS to confirm viability of mechanical structure, and integrity of internal cabling scheme (HV, signal, calibration).
- 2025-2026 (LS3): analysis of fused silica samples irradiated in Run 3. Procurement of final fused silica rods, and ATLAS and CMS construction of four production detectors, two per experiment (with the choice of joint or separate projects deferred until further discussions with the experiments). HL-LHC upgrades of TAXNs and installation of new cranes, culminating in transport tests in Points 1 and 5 with the prototype ZDC detector.
- 2027: joint SPS testbeam to validate operational readiness and initial working points for the production detectors (using measurements with variable energy and position).
- Late 2028 (potentially late 2027): installation of detectors in the ATLAS and CMS TAXNs in the technical stop preceding the first heavy ion run.

The project was already endorsed by both ATLAS and CMS collaborations, thanks to successful reviews passed around the end of 2020 The first step of the project organization consisted in the drafting of a Product Breakdown Structure (PBS), representing the hierarchical tree structure of the deliverables that have an associate CORE cost. The PBS directly seeds the Work Breakdown Structure , WBS, that identifies the tasks required to realize each of the project deliverables. Each WBS task has an unique WBS number defined in a way that can be directly associated to a PBS item.

The tasks and the scheduling are developed and managed by the respective Level-2 and Level-3 coordinators under the supervision of the Project Manager and of the Technical Coordinator, who are responsible for the complete project schedule. The WBS is organized via Microsoft Project.

References

[1] Photo-nuclear dijet production in ultra-peripheral Pb+Pb collisions. Technical Report ATLAS-CONF-2017-011, CERN, Geneva, Feb 2017.

[2] First measurement of the forward rapidity gap distribution in pPb collisions at $\sqrt{s_{NN}} =$ 8.16 TeV. 6 2020.